Journal of Materials Chemistry A

PAPER

Cite this: J. Mater. Chem. A, 2019, 7, 11127

pH-Modulated luminescence switching in a Eu-MOF: rapid detection of acidic amino acids†

Yifang Zhao, Meng-Yan Wan, Jian-Ping Bai, Heng Zeng, Weigang Lu and Dan Li *

Received 11th January 2019
Accepted 2nd April 2019

DOI: 10.1039/c9ta00384c

rsc.li/materials-a

Single-emission probes have demonstrated limited application in complex systems because the signal can be easily disrupted by many non-analyte factors. MOF-based luminescence sensors have been widely explored due to their structural abundance and tunability. Herein, we report a dual-emitting Eu-MOF (**1**), constructed by $Eu(NO_3)_3$ and 2,6-naphthalenedicarboxylic acid (H_2NDC), exhibiting a specific luminescence switching between red and blue within a pH range of 3 to 4. Through the study of single-crystal to single-crystal (SC–SC) transformation, the switching mechanism was proposed to involve the displacement of the coordinated DMF by water molecules and the slight elongation of the Eu–O bond to the ligand. These tiny changes in the local coordination environment might hinder the energy transfer from the ligand to the metal, therefore quenching the luminescence of the Eu ion and enhancing that of the ligand. With the specific pH-modulated luminescence switching property, **1** could be used as a short-range pH sensor and applied in the rapid detection of aspartic (Asp) and glutamic (Glu) acids amongst other amino acids.

1. Introduction

Amino acids, the fundamental units of polypeptides and proteins, play a wide variety of roles in the growth and development of living organisms.[1] The detection of certain amino acids is important for food safety, human nutrition and diagnosis of diseases.[2,3] For example, aspartic acid (Asp) is an endogenous amino acid for human growth.[4] It exists in the neuroendocrine tissues and plays a vital role in the early formation and growth of organisms. Recent studies show that a certain level of aspartic acid in cells is requisite for the process of respiration and cell proliferation.[5,6] So the detection of abnormal aspartic levels could be used as an early diagnosis of tumours. Amongst the traditional detection techniques, including colorimetric[7] and electrochemical methods,[8] the luminescence-based sensing of amino acids has been brought into focus as it is a facile, rapid, and highly sensitive method. Until now, a variety of studies based on metal complexes,[9,10] crown ethers,[11] polymers,[12] and so on[10,13] have been reported for the detection of amino acids. However, materials with high selectivity are still rare, as amino acids share the same functional groups—amino groups and carboxylic groups. The exploration of sensors for certain amino acids with high sensitivity and selectivity is still a challenge and urgently needed.

Metal–organic frameworks (MOFs), as a new type of porous crystalline hybrid materials,[14] have exhibited potential applications in various fields, including gas storage,[15] catalysis,[16] drug delivery,[17] and smart sensing.[18] Over the past few years, MOF-based luminescence sensors[19] have been largely explored for the detection of ionic species,[20] small molecules,[21] volatile organic compounds (VOCs),[22] explosives,[23] and biologically related molecules,[24–28] as they can be modified with specific groups to interact with the guests in their confined spaces.[29] Besides, the pore sizes and shapes of MOFs can be optimized to match the sizes of guests, achieving size selectivity. On the other hand, the luminescence of MOFs may originate from organic ligands, metal ions (*e.g.*, lanthanide ions), guest molecules, or a combination of the above, which makes MOF materials excellent self-calibrating sensors through dual- or multiple-emissions.[30] In the field of detecting amino acids, most studies are focusing on cysteine (Cys) and homocysteine (Hcy), as they have specific thiol groups.[26,31] In addition, Moorthy's group reported the synthesis of a homochiral fluorescent Zn-MOF, which was used for the selective sensing of histidine (His) in water.[24] They concluded that the charge-transfer interaction with the cationic imidazolium ring of His is the main reason for the fluorescence quenching of the pyrene-based MOF. Moreover, amino acid-triggered destruction of MOFs was used for the detection of small-sized amino acids, glycine (Gly) and serine (Ser).[32] To date, only a limited number of amino acids can be detected specifically.

College of Chemistry and Materials Science, Jinan University, Guangzhou 510632, P. R. China. E-mail: danli@jnu.edu.cn

† Electronic supplementary information (ESI) available: Physical measurements and crystal structure data. CCDC 1888969, 1888970. For ESI and crystallographic data in CIF or other electronic format see DOI: 10.1039/c9ta00384c

Compared with transition-metal MOFs, lanthanide MOFs (Ln-MOFs)[33] are more attractive candidates as luminescence sensors because the sharp and characteristic emissions of Ln ions can be modulated by analyte–ligand and/or analyte–metal interactions. Indeed, Ln-MOFs have been extensively applied in sensing ions,[34] VOCs,[35] biomarkers,[27,28] and so on.[36,37] The majority of Ln-MOFs exhibit single emissions and their "turn-on" or "turn-off" upon the encapsulation of guests can be used for sensing.[38] However, such monochromatic luminescence could be easily influenced by many non-analyte factors, such as instrumental error, background luminescence, *etc.*[39] Recently, a composite strategy to construct dichromatic materials was developed by incorporating luminescent molecules as reference emission. Upon loading perylene in ZJU-88, Qian's group obtained a temperature-sensitive dual-emitting material, which is more sensitive and reliable than the monochromatic MOF.[40] Still, the possibility of dye leaching and channel blocking might hinder the applications of these kinds of composites. Therefore, MOFs with intrinsic dual-emission luminescence are much desired in this kind of application.

It is known that the luminescence of lanthanides could be easily quenched by high-energy vibrations, particularly O–H.[41] In this regard, H_2O is a good quencher, which should be avoided in the construction of luminescent Ln-MOFs. Nevertheless, the quenching effects of the vibrations could be utilized in the sensing application.[22,42] In 2008, Chen's group reported that a prototype MOF, namely Tb(BTC), exhibited high-sensitivity sensing of fluoride anions. They speculated that the quenching effect of O–H stretching within the terminal methanol on the luminescence intensity of Tb could be tuned by the hydrogen-bonding interaction with the fluoride anion.[42] In 2013, Song's group synthesized a new Eu-MOF with a selective luminescence "turn-on" response to dimethylformamide (DMF) vapour. Besides the DMF–ligand interaction, they assumed that replacing water molecules around the Eu centre with DMF molecules might also trigger the enhancement of Eu emission.[22]

Herein, we report a dual-emission Eu-MOF (**1**) constructed from 2,6-naphthalenedicarboxylic acid (H_2NDC).[43] It exhibits a luminescence switching between red and blue triggered by pH over a range of 3 to 4 (Scheme 1). Through the study of single-crystal to single-crystal (SC–SC) transformation, a mechanism is proposed and the switching behaviour is attributed to the rapid replacement of DMF with water molecules and the slight elongation of the Eu–O bond, which possibly hinder the energy transfer from the ligand to the metal, resulting in a decreased emission of Eu^{3+} and enhanced emission of the ligand at the same time. Owing to its unique pH-induced luminescence switching property, **1** shows great potential in the rapid detection of Asp and Glu amongst other amino acids.

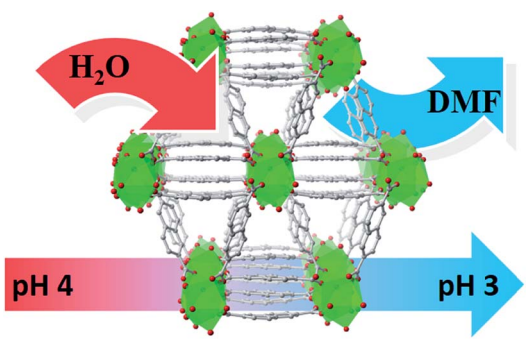

Scheme 1 pH-Modulated luminescence switching of **1**.

2. Experimental

2.1 Preparation of 1 and 2

All the reagents and solvents for synthesis and measurement were purchased from commercial sources and used as received. **1** was prepared by solvothermal reaction according to a modified literature[43] method. Specifically, a solution containing a mixture of $Eu(NO_3)_2 \cdot 6H_2O$ (0.02 mmol), 2,6-naphthalenedicarboxylic acid (H_2NDC, 0.03 mmol), H_2O (1 mL), MeOH (2 mL) and DMF (4 mL) was sealed in a Pyrex glass tube and heated in an oven at 95 °C for 24 h, and then cooled to room temperature at a rate of 5 °C h^{-1}. Colorless columnar crystals were obtained (yield: 52% based on Eu salt). **1** was washed with deionized water three times and then filtered before measurement. A single crystal of **2** was obtained by immersing a single crystal of **1** in an aqueous HCl solution of pH 3 until the emission colour changed under UV light.

2.2 Characterization

Single crystal X-ray diffraction (SXRD) data were collected on an Oxford Cryo stream system with an XtaLAB PRO MM007-DW diffractometer (Cu-Kα, graphite monochromator, λ = 1.54 Å) at 150.0 K. Data reduction was performed using the CryAlisPro program, by Gaussian adsorption correction. The structures were solved and refined using the SHELX program. The PLATON/SQUEEZE program was used to remove scattering contributions from disordered guest molecules and to produce solvent-free diffraction intensities, which were used in the final structure refinement. CCDC-1888970 (**1**) and CCDC-1888969 (**2**) contain the ESI crystallographic data for this paper.† Powder X-ray diffraction (PXRD) patterns were collected on a Rigaku Ultima IV diffractometer with Cu Kα radiation (λ = 1.5418 Å) in a step of 0.02° under the tube conditions of 40 kV and 40 mA. The Pawley refinement of **1** immersed in water was carried out using the Reflex module of Material Studio 7.0. The Fourier transform infrared (FT-IR) spectra were measured using a Thermo Scientific FT-IR Nicolet iS10 spectrophotometer. The UV-Vis spectra of the aqueous solutions of amino acids were recorded on a Bio-Logic MOS-500 multifunctional circular dichroism spectrometer. Photoluminescence (PL) spectra were recorded on an Edinburgh FLS980 lifetime and steady state spectrometer. The absolute quantum yield was measured at room temperature by employing a Hamamatsu C11347-11 absolute PL quantum yield spectrometer. The thermogravimetric analysis (TGA) was carried out on a TGA 2 with a heating rate of 10 °C min^{-1} from 40 to 800 °C in a N_2 atmosphere.

2.3 Luminescence measurements

The luminescence studies were performed by using aqueous suspensions of **1** at 298 K. Typically, a suspension was prepared by dispersing the finely ground **1** (1.5 mg) into water (5 mL) and sonicated for 1 min. The luminescence spectra of the resultant suspensions were recorded upon excitation at 350 nm. Each test was repeated five times. Similarly, **1** was added into aqueous HCl solutions (pH 1 to 6 and 3.90 to 3.00) or aqueous solutions containing Asp and Glu (0.1 mM to 1.2 mM) as well as other amino acids (1.0 mM). The luminescence spectra of these suspensions were recorded after being sonicated for 1 min. **1** was regenerated by immersion in ethanol.

3. Results and discussion

3.1 Preparation and characterization

The SXRD study revealed that **1** crystallized in the monoclinic space group $P2_1/n$. As shown in Fig. 1a, one NDC ligand in the as-synthesized framework is bonded to four Eu ions in two modes: a bidentate bridging mode (mode I) and a bidentate chelating-bridging mode (mode II). The ligand in the first mode acts as a bridge with four oxygen atoms bonded to four Eu ions individually; while in the second mode, besides acting as a bridge, the ligand also shares two oxygen atoms with one Eu ion in a chelating fashion. The eight-coordinated Eu centre is surrounded by one coordinated DMF molecule, five monodentate carboxylates and one chelating carboxylate of NDC ligands. Two Eu ions form an edge-sharing Eu_2 unit through a chelating carboxylate and further extend to a one-dimensional (1D) Eu chain along the crystallographic *c* axis through four bridging carboxylates in mode I. Significantly, besides constructing the Eu chain, the NDC ligands in mode I interconnect the neighbouring Eu chains into a two-dimensional (2D) "double-decker" layer in the *ac* plane. The NDC ligands in mode II act as pillars and link these layers to form a three-dimensional (3D) framework. Interestingly, the structure of **1** is slightly different from that of FJU6, which was synthesized by a similar procedure.[41] They have the same 3D pillar-supported double-decker network, however, the bridging water molecules between the Eu_2 units are not observed by SXRD in our structure. And the distances between Eu ions in **1** are 3.91 Å and 5.02 Å, as opposed to 4.092 Å and 4.841 Å in FJU6.

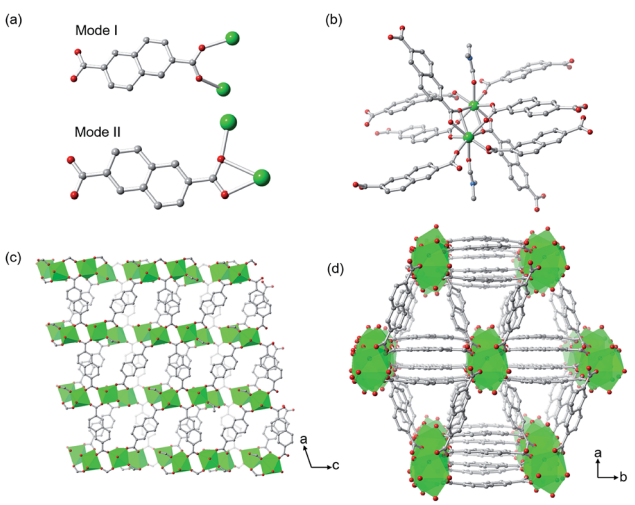

Fig. 1 (a) The coordination modes of NDC ligands and Eu ions; (b) the coordination states of the Eu pair in **1**; (c) a packed 2D layer along the *b* axis; (d) a 3D framework of **1** viewed along the *c* axis. The DMF molecules were omitted for clarity. The green balls represent the Eu ions, gray ones are carbon atoms, and the red ones are oxygen atoms.

The thermal stability of **1** was tested by TGA in a temperature range of 40 to 800 °C under a flow of N_2. As shown in Fig. S7,† **1** exhibits a continuous weight loss of 18.8% from 60 to 300 °C, which corresponds to the release of one lattice DMF and two coordinated DMF molecules, and then a sharp weight loss of 51% from 460 to 550 °C which is attributed to the decomposition of the structure. The chemical stability of **1** in water and HCl solutions was validated by the PXRD of the bulk sample after being immersed in water and HCl solutions (pH 1 to 6) for 24 h. As shown in Fig. S4 and S5,† the diffraction pattern of the as-synthesized **1** matched well with the simulated one from the SXRD data, confirming the phase purity of **1**. Although the peaks shifted after immersion in water for 24 h, they could be reinstated once re-immersed in DMF, indicating that the framework can transform reversibly, which is common in MOF-based materials.[44,45] The PXRD patterns of the HCl-treated **1** (pH 3 to 7) were identical to the one immersed in water, which implied that **1** was stable under these conditions. However, the framework was partially destroyed in pH 2 solution and completely decomposed in pH 1 solution (Fig. S11†). The PXRD analysis could be further confirmed by the FT-IR study (Fig. S12†). Compared with the FT-IR spectra of as-synthesized **1**, most peaks of the FT-IR spectra of the HCl-treated samples (pH 4 and 3) were retained except for the one at 1670 cm^{-1} (representing the absorption of $C{=}O_{DMF}$ bond stretching). And the absorption peaks at around 1720–1680 cm^{-1} as well as 3500–2500 cm^{-1} appeared at pH 2, presumably from the protonated carbonyl group of the free ligand, indicating that the MOF was partially decomposed.[41] Thus, it can be concluded that **1** exhibits good thermal and chemical stability, which is important for further application in aqueous solutions.

A comprehensive study of the photoluminescence (PL) properties was carried out. First, the PL spectra of as-synthesized samples, H_2NDC, and the HCl-treated samples were measured at room temperature. As shown in Fig. S8 to S10,† under excitation of 350 nm, a broad band in the range of 400–600 nm is observed in the emission spectrum of H_2NDC, while the spectrum of **1** exhibits the well-resolved characteristic emissions of Eu^{3+} with peaks at 578, 590, 611, 651 and 697 nm,[46] attributed to the $^5D_0 \rightarrow {}^7F_J$ ($J = 0$, 1, 2, 3, and 4) transitions of the Eu ion, respectively. The absence of the emission peak of the ligand in **1** indicates that the ligand can sensitize the luminescent Eu^{3+} effectively by the ligand-to-metal energy transfer process.[47] The luminescence quantum yield of **1** in the solid state was measured to be 42.1% (excitation at 350 nm), further confirming the sensitization ability of the ligand. Besides, the excitation and the emission spectra of the suspensions of **1** show no obvious changes compared with the solid state, indicating the high stability of **1** in water. In addition, the emission spectra of the samples were also recorded after being immersed in acidic solutions with pH from 3 to 6 for 24 h. As shown in Fig. 2, the emission spectra of

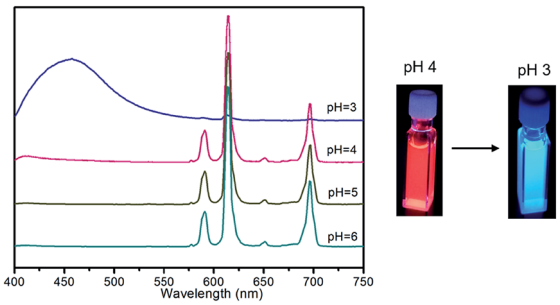

Fig. 2 Emission spectra of **1** after immersion in HCl solutions of pH 3 to 6. Photographs are shown for pH 4 and 3 under 365 nm UV light.

the samples in the pH range of 4 to 6 retain the characteristic peaks of Eu^{3+} and there are no significant changes in peak intensities. However, the colour of the MOF changed from red to blue once immersed in a pH 3 solution (Fig. 2).

3.2 pH-Modulated luminescence switching of 1

For better understanding the colour change of **1** in the pH range of 4 to 3, the emission spectra of the samples were recorded and analysed after being deposited into HCl solutions with precise pH values from 3.90 to 3.00. As shown in Fig. 3, the PL intensity of Eu^{3+} decreases while that of the ligand increases gradually with the lowering of pH. Herein, the relative intensity at 615 nm (I/I_0) first declines slowly within pH 3.90 to 3.50, and then drops quickly to zero, while the relative intensity at 459 nm ($I/I_{3.00}$) shows an opposite trend. It is concluded that **1** is very sensitive to the pH values in the range of 3 to 4 and can be potentially used as a short-range pH sensor.

XRD studies were performed to explore the mechanism of this specific luminescence switching. The PXRD patterns of the samples remain unchanged after being immersed in pH 3 to 4 solutions, implying that the switching of the PL intensity of **1** comes from the minor changes in the local structures instead of the whole framework. So the SXRD data were collected for the single crystal after being immersed in an acidic solution (pH 3) for several seconds. Compared with the as-synthesized structure **1**, **2** retains the 3D pillar-supported double-decker network, however, the coordination environments of Eu ions are slightly changed. Besides the five monodentate bridging carboxylates and one chelating carboxylate of NDC ligands, the Eu ion is coordinated to one bridging water molecule and one terminal water molecule, instead of one DMF molecule before HCl treatment (Fig. 4). The ligands reorient slightly and the bond lengths of Eu–O are longer than those in the original framework (Tables S2 and S3†). In addition, the distances of the Eu···Eu··· Eu sequence have adjusted to 4.04 and 4.72 Å (Fig. S3†). The pH-induced PL switching mechanism is proposed as follows: in the as-synthesized **1**, there is an effective energy transfer from the ligand to the Eu ion (antenna effect) and it exhibits a characteristic emission of the Eu ion (red). This property is not affected in the pH range of 4 to 6. However, when in the pH range of 3 to 4, the coordinated DMF molecules are rapidly replaced by water molecules and the bond lengths of Eu–O are slightly increased. These changes might weaken the energy transfer from the ligand to the Eu ion and result in the emission quenching of the Eu ion (red) and the emission enhancement of the ligand (blue). So the luminescence of **1** changes from red to blue.

The switching mechanism was further verified by additional experiments. Firstly, the emission properties of the sample stored in deionized water for 6 months were measured, as shown in Fig. S13,† and no obvious changes were observed compared with the original one. This indicates that water molecules hardly replace the coordinated DMF molecules under neutral conditions. Besides, the emission spectra of the HCl-treated samples after immersion into ethanol (Fig. S15†) show that the original luminescence can be recovered once the coordinated water molecules are replaced by ethanol molecules, which indicates that the material can be easily regenerated. What's more, the emission intensity of **1** at 615 nm was measured as a function of time after addition into an acidic

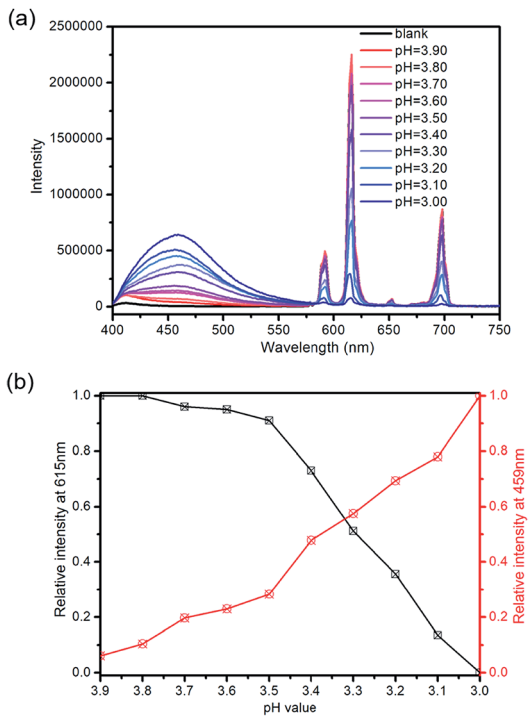

Fig. 3 (a) Emission spectra (λ_{ex} = 350 nm) of the aqueous solutions of **1** at different pHs. (b) The relative intensities at 615 nm (I/I_0) and 459 nm ($I/I_{3.00}$) *versus* pH.

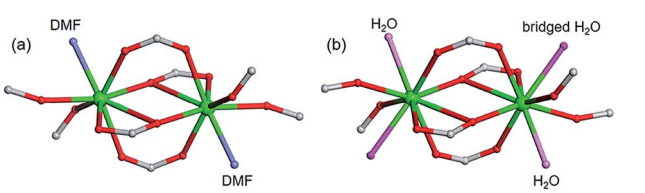

Fig. 4 The coordination states of Eu before (**1**, a) and after (**2**, b) HCl-treatment. Key: purple, O in DMF; pink, O in terminal H_2O; magenta, O in bridging H_2O.

solution (pH 3.2). As shown in Fig. S16,† the emission of the Eu ion is completely quenched within 1 min, even though the MOF is not nano-sized. These experiments reveal that the DMF molecules can be replaced rapidly in acidic solutions of pH less than 4.

3.3 Sensing of acidic amino acids

The specific and rapid luminescence response to pH of **1** encouraged us to test it as a short-range pH sensor. According to the literature, pH sensors usually contain functional groups from ligands that can bind either H^+ or OH^- at certain pH.[48] Differently, the specific pH sensing properties of **1** are due to the changing coordination environment of the metal ion under different pH conditions. Bearing this in mind, acidic amino acids (Asp and Glu) were chosen for the test as their aqueous solutions at certain concentrations are in a pH range between 3 and 4 (Table S5†). As expected, **1** shows an excellent luminescence response specifically to these two acidic amino acids. In the luminescent titration experiments, the emission intensity of **1** starts to change upon the addition of 0.1 mM acidic amino acids. A gradual decrease in the luminescence intensity of the Eu ion and increase in that of the ligand are observed with increasing concentration of Asp or Glu (Fig. 5 and S19†). The emission at 615 nm is significantly quenched upon addition of 1.2 mM Asp or Glu aqueous solution with a quenching efficiency of 92% and 79.9%, respectively. The relative intensity of I/I_0 at 615 nm can be fitted linearly with the concentrations, however, the relative intensities of I_{459}/I_{615} and I_0/I at 615 nm show a nonlinear correlation. To further investigate the sensing performance of **1**, the luminescence quenching efficiency at 615 nm is quantitatively explained by the Stern–Volmer (S–V) equation[49] at low concentrations. For Asp, the linear correlation can be fitted to $I_0/I = 1 + 1.4043[C]$ at 0 to 0.4 mM. The detection limit (LOD) is estimated to be 21 μM (LOD = $3\sigma/k$, k: slope, σ: standard deviation). And the LOD for Glu is 22.4 μM. Moreover, the emission colour of **1** changes within one minute after

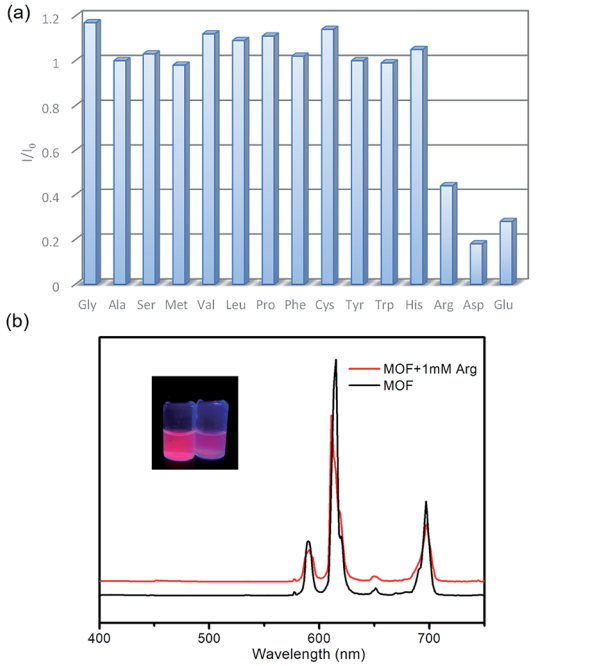

Fig. 6 (a) Quenching ratio (I/I_0) of the suspensions of **1** for different amino acids (1.0 mM); (b) emission spectra of **1** and **1** in 1.0 mM Arg solution. The inset shows the corresponding photograph under 365 nm UV light.

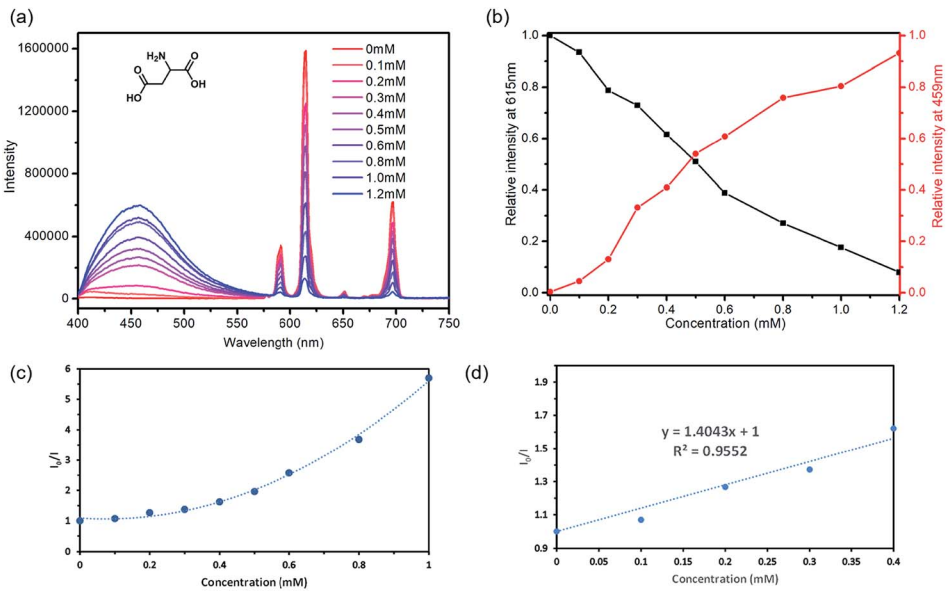

Fig. 5 (a) Emission spectra of **1** at different concentrations of Asp in water; and (b) the corresponding plot of the relative intensity at 615 nm and 459 nm as a function of concentration. The relative intensity at 615 nm is calculated by I/I_0 (I_0 is the peak intensity at 615 nm for the as-synthesized sample). The relative intensity at 459 nm is calculated by $I/I_{3.00}$ ($I_{3.00}$ is the peak intensity at 459 nm for the HCl-treated samples at pH 3.00); (c) Stern–Volmer (S–V) plot of **1** in Asp, and (d) the corresponding linear fitting at low concentrations.

immersion in Asp or Glu solutions. These results suggest that **1** could be ideal for short-range pH sensing due to its striking luminescence change, rapid response, and low detection concentration.

The emission switching behaviour of **1** was also tested on other amino acids, including small (alanine (Ala) and glycine (Gly)), nucleophilic (serine (Ser) and cysteine (Cys)), hydrophobic (valine (Val), leucine (Leu) and proline (Pro)), aromatic (phenylalanine (Phe), tyrosine (Tyr), and tryptophan (Trp)), and basic (arginine (Arg) and histidine (His)) amino acids. Similarly, the finely ground samples of **1** were added into aqueous solutions of these amino acids (1.0 mM) and sonicated for 1 min. The emission signals at 615 nm were monitored before and after the addition. As demonstrated by the quenching efficiencies in Fig. 6, most amino acids have little effect on the emission properties of **1**. Although Arg can quench the emission of Eu^{3+} as much as 56%. Asp and Glu not only quench the emission of Eu^{3+}, but also enhance that of the ligand. Therefore, **1** can effectively differentiate these two acidic amino acids from other amino acids by displaying a specific dual-emission luminescence switching behaviour.

4. Conclusions

In summary, we discovered a dual-emission Eu-MOF (**1**) with a specific luminescence switching behaviour in a pH range between 3 and 4. A thorough experimental study suggested that it could be an excellent sensor for the rapid detection of acidic amino acids (Asp and Glu) amongst other amino acids for the first time. Through the study of SC–SC transformation, the luminescence switching mechanism is attributed to the rapid coordination of water molecules and the slight elongation of the Eu–O bond, which we believe may weaken the energy transfer from the ligand to the Eu ion and therefore result in the luminescence quenching of the Eu ion as well as the luminescence enhancing of the ligand. Different from other pH sensors, the specific sensing properties of **1** are related to the coordination state of the Eu ion, as the tiny changes in the local coordination environment could largely influence its physical properties. This concept may provide some insight into the design of coordination polymers toward high performance in various sensing applications.

Conflicts of interest

There are no conflicts to declare.

Acknowledgements

The work was financially supported by the National Natural Science Foundation of China (No. 21731002 and 91222202).

Notes and references

1 G. C. Barrett and D. T. Elmore, *Amino Acids and Peptides*, Cambridge University Press, 1998.
2 M. Friedman, *J. Agric. Food Chem.*, 1999, **47**, 3457–3479.
3 A. D'Aniello, A. Vetere, G. H. Fisher, G. Cusano, M. Chavez and L. Petrucelli, *Brain Res.*, 1992, **592**, 44–48.
4 A. D'Aniello, *Brain Res. Rev.*, 2007, **53**, 215–234.
5 K. Birsoy, T. Wang, W. W. Chen, E. Freinkman, M. Abu-Remaileh and D. M. Sabatini, *Cell*, 2015, **162**, 540–551.
6 L. B. Sullivan, D. Y. Gui, A. M. Hosios, L. N. Bush, E. Freinkman and M. G. Vander Heiden, *Cell*, 2015, **162**, 552–563.
7 J. F. Folmer-Andersen, V. M. Lynch and E. V. Anslyn, *Chemistry*, 2005, **11**, 5319–5326.
8 M. S. Yao, W. X. Tang, G. E. Wang, B. Nath and G. Xu, *Adv. Mater.*, 2016, **28**, 5229–5234.
9 J. Wang, H.-B. Liu, Z. Tong and C.-S. Ha, *Coord. Chem. Rev.*, 2015, **303**, 139–184.
10 M. Zhang, M. L. Saha, M. Wang, Z. Zhou, B. Song, C. Lu, X. Yan, X. Li, F. Huang, S. Yin and P. J. Stang, *J. Am. Chem. Soc.*, 2017, **139**(14), 5067–5074.
11 J. Du, Z. Huang, X. Q. Yu and L. Pu, *Chem. Commun.*, 2013, **49**, 5399–5401.
12 H. N. Kim, Z. Guo, W. Zhu, J. Yoon and H. Tian, *Chem. Soc. Rev.*, 2011, **40**, 79–93.
13 D. E. Barry, D. F. Caffrey and T. Gunnlaugsson, *Chem. Soc. Rev.*, 2016, **45**, 3244–3274.
14 H. Furukawa, K. E. Cordova, M. O'Keeffe and O. M. Yaghi, *Science*, 2013, **341**, 1230444.
15 J. Sculley, D. Yuan and H.-C. Zhou, *Energy Environ. Sci.*, 2011, **4**, 2721–2735.
16 J. Liu, L. Chen, H. Cui, J. Zhang, L. Zhang and C. Y. Su, *Chem. Soc. Rev.*, 2014, **43**, 6011–6061.
17 P. Horcajada, T. Chalati, C. Serre, B. Gillet, C. Sebrie, T. Baati, J. F. Eubank, D. Heurtaux, P. Clayette, C. Kreuz, J.-S. Chang, Y. K. Hwang, V. Marsaud, P.-N. Bories, L. Cynober, S. Gil, G. Férey, P. Couvreur and R. Gref, *Nat. Mater.*, 2009, **9**, 172.
18 D. Wu, A. C. Sedgwick, T. Gunnlaugsson, E. U. Akkaya, J. Yoon and T. D. James, *Chem. Soc. Rev.*, 2017, **46**, 7105–7123.
19 W. P. Lustig, S. Mukherjee, N. D. Rudd, A. V. Desai, J. Li and S. K. Ghosh, *Chem. Soc. Rev.*, 2017, **46**, 3242–3285.
20 L. Li, S. Shen, R. Lin, Y. Bai and H. Liu, *Chem. Commun.*, 2017, **53**, 9986–9989.
21 Q. Li, J. Wu, L. Huang, J. Gao, H. Zhou, Y. Shi, Q. Pan, G. Zhang, Y. Du and W. Liang, *J. Mater. Chem. A*, 2018, **6**, 12115–12124.
22 J.-H. Wang, M. Li and D. Li, *Chem. Sci.*, 2013, **4**, 1793–1801.
23 M. Rieger, M. Wittek, P. Scherer, S. Löbbecke and K. Müller-Buschbaum, *Adv. Funct. Mater.*, 2018, **28**, 1704250.
24 P. Chandrasekhar, A. Mukhopadhyay, G. Savitha and J. N. Moorthy, *Chem. Sci.*, 2016, **7**, 3085–3091.
25 B. Wang, X. L. Lv, D. Feng, L. H. Xie, J. Zhang, M. Li, Y. Xie, J. R. Li and H. C. Zhou, *J. Am. Chem. Soc.*, 2016, **138**, 6204–6216.
26 J. Wang, Y. Liu, M. Jiang, Y. Li, L. Xia and P. Wu, *Chem. Commun.*, 2018, **54**, 1004–1007.
27 S. Y. Zhang, W. Shi, P. Cheng and M. J. Zaworotko, *J. Am. Chem. Soc.*, 2015, **137**, 12203–12206.

28 S. Wu, Y. Lin, J. Liu, W. Shi, G. Yang and P. Cheng, *Adv. Funct. Mater.*, 2018, **28**, 1707169.
29 W. Lu, Z. Wei, Z.-Y. Gu, T.-F. Liu, J. Park, J. Park, J. Tian, M. Zhang, Q. Zhang, T. Gentle III, M. Bosch and H.-C. Zhou, *Chem. Soc. Rev.*, 2014, **43**, 5561–5593.
30 H. Zhao, J. Ni, J. J. Zhang, S. Q. Liu, Y. J. Sun, H. Zhou, Y. Q. Li and C. Y. Duan, *Chem. Sci.*, 2018, **9**, 2918–2926.
31 H. Li, X. Feng, Y. Guo, D. Chen, R. Li, X. Ren, X. Jiang, Y. Dong and B. Wang, *Sci. Rep.*, 2014, **4**, 4366.
32 W. Li, X. Qi, C. Y. Zhao, X. F. Xu, A. N. Tang and D. M. Kong, *ACS Appl. Mater. Interfaces*, 2017, **9**, 236–243.
33 J. Rocha, L. D. Carlos, F. A. Paz and D. Ananias, *Chem. Soc. Rev.*, 2011, **40**, 926–940.
34 H. Xu, C. S. Cao, X. M. Kang and B. Zhao, *Dalton Trans.*, 2016, **45**, 18003–18017.
35 T. Gong, P. Li, Q. Sui, J. Chen, J. Xu and E.-Q. Gao, *J. Mater. Chem. A*, 2018, **6**, 9236–9244.
36 Y.-J. Li, Y.-L. Wang and Q.-Y. Liu, *Inorg. Chem.*, 2017, **56**, 2159–2164.
37 R. He, Y.-L. Wang, H.-F. Ma, S.-G. Yin and Q.-Y. Liu, *Dyes Pigm.*, 2018, **151**, 342–347.
38 D. Yue, D. Zhao, J. Zhang, L. Zhang, K. Jiang, X. Zhang, Y. Cui, Y. Yang, B. Chen and G. Qian, *Chem. Commun.*, 2017, **53**, 11221–11224.
39 X. Huang, J. Song, B. C. Yung, X. Huang, Y. Xiong and X. Chen, *Chem. Soc. Rev.*, 2018, **47**, 2873–2920.
40 Y. Cui, R. Song, J. Yu, M. Liu, Z. Wang, C. Wu, Y. Yang, Z. Wang, B. Chen and G. Qian, *Adv. Mater.*, 2015, **27**, 1420–1425.
41 A. Beeby, I. M. Clarkson, R. S. Dickins, S. Faulkner, D. Parker, L. Royle, A. S. de Sousa, J. A. Gareth Williams and M. Woods, *J. Chem. Soc., Perkin Trans. 2*, 1999, 493–504.
42 B. Chen, L. Wang, F. Zapata, G. Qian and E. B. Lobkovsky, *J. Am. Chem. Soc.*, 2008, **130**, 6718–6719.
43 Y.-H. Liu and P.-H. Chien, *CrystEngComm*, 2014, **16**, 8852–8862.
44 A. X. Zhu, Q. Y. Yang, A. Kumar, C. Crowley, S. Mukherjee, K. J. Chen, S. Q. Wang, D. O'Nolan, M. Shivanna and M. J. Zaworotko, *J. Am. Chem. Soc.*, 2018, **140**, 15572–15576.
45 C. X. Bezuidenhout, V. J. Smith, C. Esterhuysen and L. J. Barbour, *J. Am. Chem. Soc.*, 2017, **139**, 5923–5929.
46 Y. Li, S. Zhang and D. Song, *Angew. Chem., Int. Ed.*, 2013, **52**, 710–713.
47 A. M. Kłonkowski, S. Lis, M. Pietraszkiewicz, Z. Hnatejko, K. Czarnobaj and M. Elbanowski, *Chem. Mater.*, 2003, **15**, 656–663.
48 H.-Y. Li, Y.-L. Wei, X.-Y. Dong, S.-Q. Zang and T. C. W. Mak, *Chem. Mater.*, 2015, **27**, 1327–1331.
49 C. Analytical Methods, *Analyst*, 1987, **112**, 199–204.